Jpn. J. Appl. Phys. Vol. 38 (1999) pp. 1564–1568
Part 1, No. 3A, March 1999

Behaviors of Excitation Cross Sections in the Intermediate Velocity Regime on Ion-Atom Collisions

Rei OKASAKA, Yoshiho SEO, Satoshi TOJO and Yasuo MATSUMURA
Department of Mechanical Physics, Kyoto University, Yoshida-Honmachi, Sakyo-ku, Kyoto 606-8501, Japan

(Received September 24, 1998; accepted for publication December 16, 1998)

We studied the behaviors of excitation cross sections and electron capture cross sections as functions of collision velocity using previous data of various collision systems. The structures peculiar to the intermediate velocity regime were recognized on the excitation cross sections. Close correlation of the excitation cross section to the electron capture cross section and a relaxation time longer than that for the electron capture process characterize the excitation process in the intermediate velocity regime. A model consisting of a two-step electron transfer process well explains the characteristics of the excitation cross sections in the intermediate velocity regime.

KEYWORDS: ion-atom collision, intermediate velocity region, excitation function, electron transfer process

1. Introduction

It is well known that a Born approximation is can be applied to the calculation of the excitation cross sections in the velocity range near the high-velocity limit of a direct excitation process of ion-atom collisions. The results obtained by a distorted wave method also are in good agreement with the experimental results for comparatively high-velocity collisions. The distorted wave method, however, is not effective for the low-velocity side of the direct excitation range, and sometimes fails to explain the complex structure appearing in this velocity range or in the range of a slightly lower velocity. A close-coupling method based on atomic or molecular wave functions is often used to explain the structure appearing in this velocity range. Many basis functions and an enormous number of calculations are needed to adequately describe the functions of the excitation cross sections against collision velocity (excitation functions) using this method.

The complex behavior as a function of collision velocity in the velocity region mentioned above is quite different from the behavior of the excitation cross section generated by the direct excitation process. The excitation process producing the complex structure, moreover, is different from the quasi-molecular interaction in the low velocity regime. We consider the velocity range where this excitation process is effective to be the intermediate velocity regime (refer to §2).

Systematic studies on He^+–He collisions[1] showed a close correlation between the excitation cross sections and the electron capture cross sections in the intermediate velocity regime. Thus we proposed a model of excitation consisting of an electron exchange process for intermediate velocity He^+–He collisions.

In this work, we studied the characteristics of the structures in the intermediate velocity regime for various collision systems of H^+–He, H^+–Na, He^+–He and H^+–H. The structures of the excitation functions peculiar to the intermediate velocity regime were also recognized. Based on the characteristics observed for the excitation and electron capture cross sections in the intermediate velocity regime, we proposed an excitation model consisting of a two-step electron transfer process, and examined the phenomenological validity of the model. When a satisfactory model is obtained for the analysis of the excitation functions, it may suggest a simplified method of calculating the excitation cross sections in the intermediate velocity regime.

2. Characteristics of the Excitation Functions in the Intermediate Velocity Regime

The intermediate velocity regime of ion-atom collisions usually indicates the velocity range where the orbit velocity of an active electron of a target atom is nearly equal to the velocity of an incident ion. From a different standpoint, we can consider the intermediate velocity regime as the velocity range in which the duration of the interaction is too long to treat the interaction as a perturbative one.[2] We also consider the duration to be too short for the collision system to form a quasi-molecular state; an active electron does not complete its orbit in the duration of the collisional interaction in the intermediate velocity regime.

Figure 1(a) shows the excitation functions of the He(3^1P) level in the H^+–He collisions.[1,3] The excitation functions of He^+ impact[1,4] and e^- impact[5] are also shown in the figure. In the case of a helium atom target, the intermediate velocity regime is about 1–3 $\times$ 10^6 m/s (ref. 1). The structure P_1 on the excitation function of H^+ impact, the maximum of which is designated by the arrow P_1, overlaps the structures of He^+ and e^- impacts and all the structures show nearly the same dependence on collision velocity. This means that the excitation mechanism producing the P_1 structure does not depend on the constitution of the impacting charged particle. Therefore, we assign the process of direct excitation in the high velocity regime as the origin of the P_1 structure. (The cross sections of electron impact in the velocity region below the peak of P_1 are small in comparison with the cross sections of heavy-particle impacts. This is due to the difference in the incident particle masses. In the intermediate velocity regime, the incident energy of the electron is small, comparable to the excitation energy of the He(3^1P) level. Most of the incident energy is expended as excitation energy and the effective collision velocity becomes much smaller than the incident velocity.)

We see another structure P_2 on the excitation function of the H^+ impact. We do not observe any appreciable structure in the low velocity regime because there is no quasi-molecular state of the H^+–He system that leads to the He(3^1P) level excitation. Based on these results, we infer that the P_2 structure is peculiar to the intermediate velocity regime.

Next we search for the structures which correspond to the P_2 peak of H^+–He collisions on excitation functions of other collision systems. The excitation functions of the Na(3p) level for H^+–Na and e^-–Na collisions are shown in Fig. 2(a).[6,7] The structure designated by the arrow P_1 on the ex-

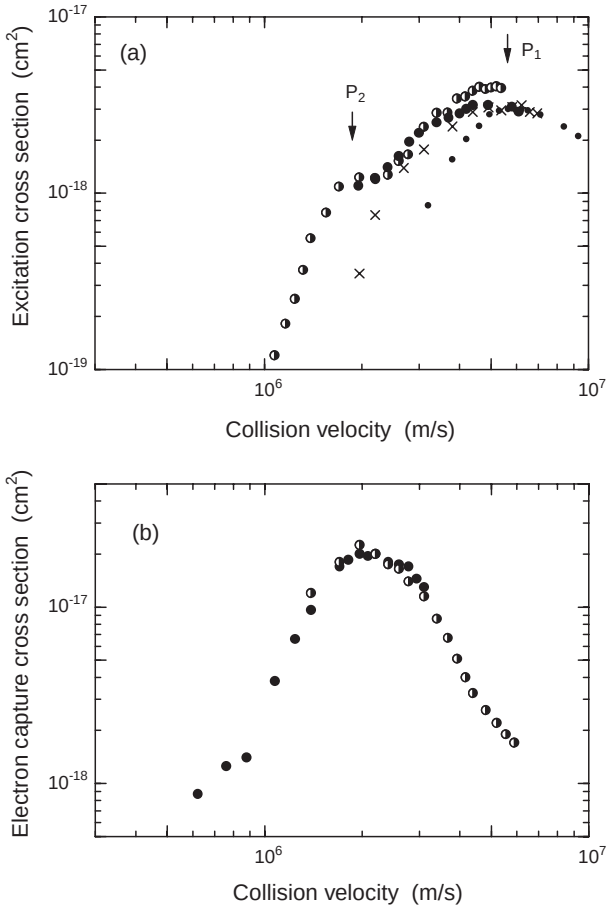

Fig. 1. Excitation cross sections of the He(3^1P) level and electron capture cross sections in the H^+-He collisions. (a) Excitation cross sections of the He(3^1P) level for H^+, He^+, and e^- impacts. H^+: solid circles,[1] half-solid circles.[3] He^+: crosses.[4] e^-: small solid circles.[5] (b) Total electron capture cross sections in the H^+–He collisions. Solid circles,[15] half-solid circles.[16]

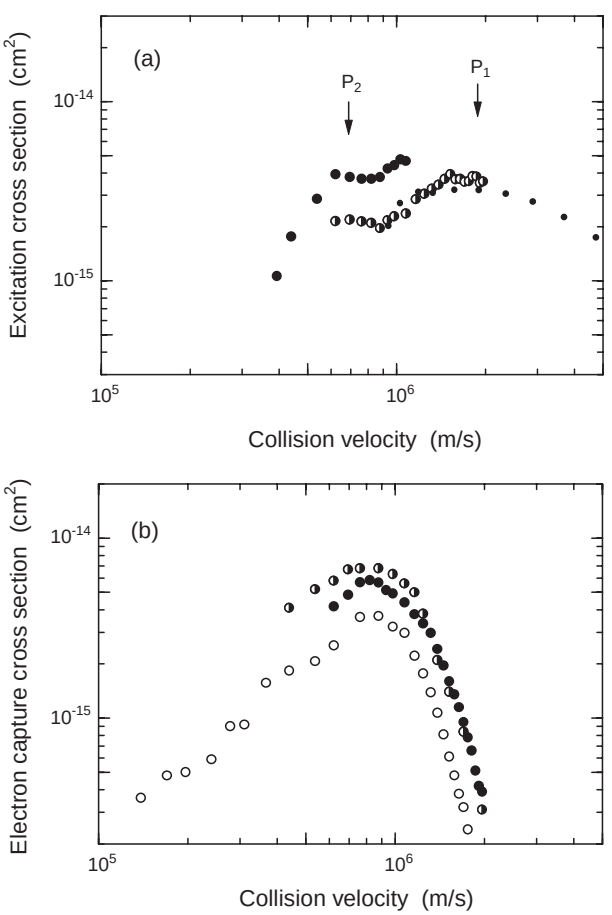

Fig. 2. Excitation cross sections of the Na(3p) level and electron capture cross sections in the H^+-Na collisions. (a) Excitation cross sections of the Na(3p) level for H^+ and e^- impacts. H^+: solid circles,[6] half-solid circles.[7] e^-: small solid circles.[8] (b) Electron capture cross sections in the H^+–Na collisions. Total electron capture: solid circles,[7] half-solid circles.[17] Capture to the H(2p) level: open circles.[18]

citation function of proton impact agrees with the profile of electron impact, and we consider the structure to be a product of the direct excitation process. Another peak, P_2, distinguished from the structure of direct excitation, is observed in the intermediate velocity regime in Fig. 2(a), similar to seen in Fig. 1(a).

The excitation function of the He(3^1P) level extended to the low velocity regime,[1,4] and the electron capture cross sections of the He(3^1P) level[1] for He^+–He collisions are shown in Fig. 3(a). We observe the structure corresponding to the peak P_2 in the intermediate velocity regime on the excitation function. The profile of peak P_2 resembles that of the first peak of the electron capture cross section, however, the entire profile of peak P_2 shifts toward the low-velocity side in comparison with the structure of the electron capture cross section. We assume, therefore, that the relaxation time required to excite an electron is longer than that required to capture the electron at the excited level. For He^+–He collisions, a channel of the quasi-molecular state that tends to the He(3^1P) level at the separated limit of the internuclear distance[9] produces a considerably large excitation cross section or electron capture cross section in the low velocity regime. There exists an antiphase oscillation between the excitation and electron capture cross sections due to by the phase-interference effect.[10]

Figure 4(a) shows the excitation functions of the H(2p) level for H^+ impact[11,12] and e^- impact.[13] The figure also includes the electron capture cross sections of the H(2p) level for the H^+–H collisions.[14] For H^+–H collisions, the velocity region of about 0.4–2×10^6 m/s corresponds to the intermediate velocity regime.[2] On the high-velocity side of Fig. 4(a), the excitation cross sections for both H^+ and e^- impacts show nearly the same dependence on collision velocity, and thus we identify the structure as P_1 produced by the direct excitation process. With a decrease of the collision velocity, the second peak P_2 appears on the excitation function, following the increase of the electron capture cross sections. The profile of peak P_2 is almost the same as that of the velocity dependence of the electron capture cross sections. The behaviors of the excitation function and the electron capture cross sections of the H($n = 2$) levels in the low velocity regime are discussed in §2.1 of ref. 2.

3. Model for the Excitation Mechanism in the Intermediate Velocity Regime

The experimental results described in §2 suggest the existence of a structure peculiar to the intermediate velocity regime of the excitation function. Close correlation is recognized between the structure and the velocity dependence of the electron capture cross section; the profile of the structure closely resembles the behavior of the electron capture

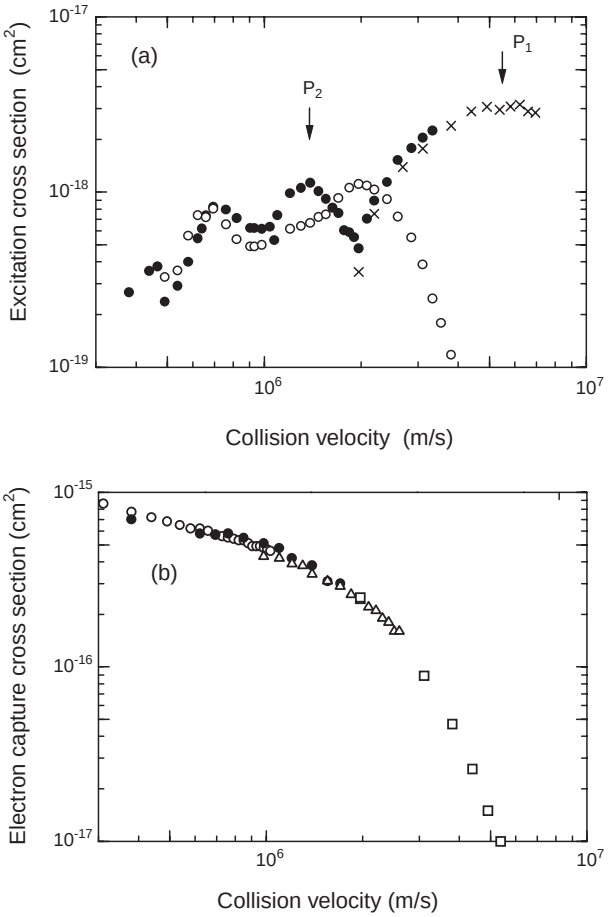

Fig. 3. Excitation and electron capture cross sections of the He(3^1P) level and electron capture cross sections in the He^+–He collisions. (a) Excitation and electron capture cross sections of the He(3^1P) level. Excitation cross sections: solid circles,[1] crosses.[4] Electron capture cross sections: open circles.[1] (b) Total electron capture cross sections. Open circles,[19] solid circles,[20] triangles,[21] squares.[22]

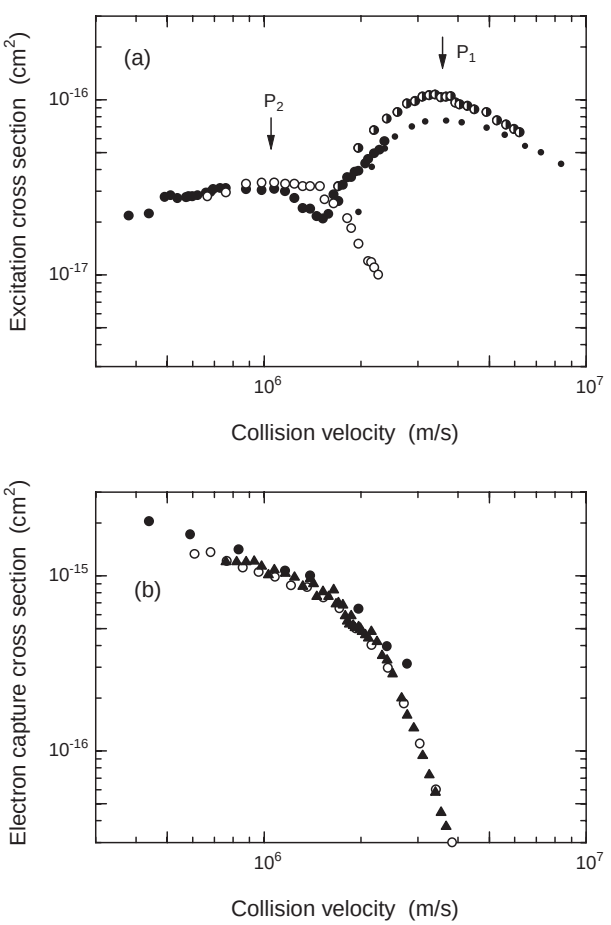

Fig. 4. Excitation and electron capture cross sections of the H(2p) level and electron capture cross sections in the H^+–H collisions. (a) Excitation cross sections of the H(2p) level for H^+ and e^- impacts. H^+: solid circles,[11] half-solid circles.[12] e^-: small solid circles.[13] Electron capture cross sections of the H(2p) level: open circles.[14] (b) Total electron capture cross sections in the H–H^+ collisions. Solid circles,[23] open circles,[24] triangles.[25]

cross section of the same level but the excitation process requires a relaxation time longer than that for electron capture. There are more details of the correlation between the excitation cross section and the electron capture cross section in the intermediate velocity regime of He^+–He collisions.[1]

i) The maximum value of the electron capture cross section is larger than that of the excitation cross section of the same level. In the low velocity regime, the excitation cross section is generally larger than the elelctron capture cross section.
ii) The velocity at which the peak of the excitation cross section appears is about 0.7 times that at which the peak of the electron capture cross section of the same level appears.
iii) Among the electron capture cross sections of the He($3^{1,3}$S,P,D) levels, the peak of the He($3^{1,3}$S) level is observed in the highest velocity region and the peaks of the He($3^{1,3}$P) and He($3^{1,3}$D) levels follow. This order of peak appearance for the electron capture cross sections agrees with that for the excitation cross sections, but is quite different from the order of peak appearance for the excitation cross sections generated by the direct excitation process in the high velocity regime.

Triplet-level excitation always accompanies an electron exchange.[1] The same behavior for both triplet-level excitation and singlet-level excitation suggests that an excitation mechanism similar to electron exchange is effective in the intermediate velocity collisions. This, along with the above-mentioned characteristics, leads us to a model of excitation which consists of a two-step electron transfer process, as follows:

$$M_1{}^+ + M_2 \underset{\text{step 1}}{\rightarrow} M_1(\text{int}) + M_2{}^+ \underset{\text{step 2}}{\rightarrow} M_1{}^+ + M_2{}^*.$$

The state M_1(int) is the intermediate state most effective for generating the $M_2{}^*$ level. We usually adopt the state with the highest production rate caused by the smallest change of internal energy at an electron transfer. Every excitation process of the examples described in §2 is considered consisting of a two-step electron tranfer process, as follows.

Case 1: $H^+ + He \rightarrow H^+ + He(3^1P)$ in Fig. 1(a),
1-1 $H^+ + He(1^1S) \rightarrow H(1s) + He^+(1s)$,
1-2 $H(1s) + He^+(1s) \rightarrow H^+ + He(3^1P)$.

Case 2: $H^+ + Na(3s) \rightarrow H^+ + Na(3p)$ in Fig. 2(a),
2-1 $H^+ + Na(3s) \rightarrow H(n=2) + Na^+$,
2-2 $H(n=2) + Na^+ \rightarrow H^+ + Na(3p)$.

Case 3: $He^+ + He \rightarrow He^+ + He(3^1P)$ in Fig. 3(a),
3-1 $He^+(1s) + He(1^1S) \rightarrow He(1s^2) + He^+(1s)$,
3-2 $He(1s^2) + He^+(1s) \rightarrow He^+(1s) + He(3^1P)$.

Case 4: $H^+ + H \rightarrow H^+ + H(2p)$ in Fig. 4(a),

4-1 $H^+ + H(1s) \rightarrow H(1s) + H^+$,

4-2 $H(1s) + H^+ \rightarrow H^+ + H(2p)$.

In our model, there are two factors which affect the behavior of the excitation cross section of $M_2{}^*$; one is the dependence of the step 1 process on collision velocity and the other is that of the step 2 process. The profile of the excitation function of $M_2{}^*$ is determined by the product of the transition probabilities of the two processes.

One-electron capture cross sections of H^+–He,[15,16] H^+–Na,[7,17,18] He^+–He,[19–22] and H^+–H[23–25] collisions are shown in Figs. 1(b), 2(b), 3(b) and 4(b), respectively. The dominant components of the above electron capture cross sections are electron capture at the H(1s), H($n = 2$), He($1s^2$) and H(1s) levels, respectively. Thus, we can regard the dependences of the cross sections on collision velocity found in Figs. 1(b), 2(b), 3(b) and 4(b) as those of processes 1-1, 2-1, 3-1 and 4-1, respectively.

We have no experimental data for the electron capture cross section of the $H(1s) + He^+(1s) \rightarrow H^+ + He(3^1P)$ process and, hence, the dependence of process 1–2 on collision velocity is not clear. Rapid decrease of the excitation cross section of the He(3^1P) level on the low-velocity side of peak P_2 in Fig. 1(a) agrees with the behavior of the electron capture cross section in the same velocity region shown in Fig. 1(b), which is nearly equal to the dependence of process 1-1 on collision velocity.

We have also no observed data for process 2-2. Process 2-2 is a sum of electron capture from the H(2s), H($2p_0$) and H($2p_{\pm1}$) levels and it may show a complex dependence on collision velocity. We assume that the decrease of the excitation function on the low-velocity side of peak P_2 in Fig. 2(a) reflects the decrease of the electron capture cross section of process 2-1 on the low-velocity side of the peak in Fig. 2(b).

Cases 3 and 4 represent the excitation processes in symmetric collision systems and processes 3-1 and 4-1 are the resonant charge exchange processes. In the resonant charge exchange process, the variation of electron capture cross section relative to collision velocity is moderate in the intermediate velocity regime as well as in the low velocity regime. It is expected that the electron capture process at the step 1 process of 3-1 or 4-1 produces no appreciable structure in the profile of the excitation function of the target atom. The electron capture cross sections of processes 3-2 and 4-2 are shown in Figs. 3(a) and 4(a) with open circles. The agreement between the behaviors of the excitation cross sections (P_2) of case 3 and 4 with those of the electron capture cross sections of processes 3-2 and 4-2, respectively, do not contradict the inference derived from our model of excitation. Profiles of P_2's in Figs. 3(a) and 4(a) shift to a low-velocity region, on the whole, in comparison with the structures of the electron capture cross sections. This, we believe, is due to the fact that the excitation mechanism of intermediate velocity collision consists of a two-step electron transfer process which requires a long interacton to complete the reaction. The characteristics observed in cases 3 and 4 are also recognized in the experimental results of Ne^+–Ne collisions[26] and we can successfully apply our model to the excitation cross sections in the intermediate velocity regime.

We conclude, as a consequence, that the behaviors of the excitation functions on the low velocity side of the structure in cases 1 and 2 reflect the dependence of the first step process on collision velocity and that, in cases 3 and 4, the dependence of the second step process determines the profile of the excitation function in the intermediate velocity regime.

4. Conclusion

The range of the intermediate velocity regime is determined mainly by the velocity of a valence electron of a target atom. Also, the interaction radius of electron capture of the incident ion may affect the velocity range where an interaction peculiar to intermediate velocity collisions is effective. The structure in the intermediate velocity regime, in many cases, overlaps the structure produced by the direct excitation process in the high velocity regime and is often regarded to be a fine structrure of direct excitation, making the reproduction of the experimental results by theoretical calculations very difficult.

In our previous paper on He^+–He collisions,[1] we reported the structure of the excitation function peculiar to the intermediate velocity regime and discussed the characteristics of the intermediate velocity collisions. In this work, the behaviors of the excitation functions in the intermediate velocity regime were studied for other collision systems. The structures peculiar to the intermediate velocity regime were also found for these collision systems. Most of the characteristics recognized in the He^+–He system were also observed in other collision systems, even the one-active-electron system.

Close correlation between the excitation cross section and the electron capture cross section and a relaxation time longer than that for the electron capture process characterize the excitation process in the intermediate velocity regime. In order to explain the observed characteristics, we proposed a model consisting of a two-step electron transfer process between an incident ion and a target atom, instead of the previous model consisting of an electron exchange process.[1] By considering the behavior of the cross section of an individual electron-transfer process in the model, we found that the structure of the excitation function reflects the behaviors of the electron capture cross sections concerned. We assume that a process, such as electron transfer from one nucleus to another, is important in the excitation process of the intermediate velocity collisions.

1) R. Okasaka, K. Kawabe, S. Kawamoto, M. Tani, H. Kuma, T. Iwai, K. Mita and A. Iwamae: Phys. Rev. A **94** (1994) 995.
2) R. Okasaka, K. Mita, S. Asada, K. Naemura and Y. Seo: Jpn. J. Appl. Phys. **38** (1999) 244.
3) J. van den Bos, G. J. Winter and F. J. de Heer: Physica **40** (1968) 357.
4) D. Hasselkamp, R. Hippler, A. Scharmann and K. H. Schartner: Z. Phys. **257** (1972) 43.
5) F. G. Donaldson, M. A. Hender and J. W. McConkey: J. Phys. B **5** (1972) 1192.
6) W. Jitschin, S. Osimitsch, D. W. Mueller, H. Reihl, R. J. Allan, O. Schöller and H. O. Lutz: J. Phys. B **19** (1986) 2299.
7) F. Aumayr, G. Lakits and H. Winter: J. Phys. B **20** (1987) 2025.
8) E. A. Enemark and A. Gallagher: Phys. Rev. A **6** (1972) 192.
9) R. Okasaka, Y. Konishi, Y. Sato and K. Fukuda: J. Phys. B **20** (1987) 3771.
10) M. Tani, A. Hishikawa and R. Okasaka: J. Phys. B **24** (1991) 1359.
11) T. Kondow, R. J. Girnius, Y. P. Chong and W. L. Fite: Phys. Rev. A **10** (1974) 1167.
12) J. T. Park, J. E. Aldag and J. M. George: Phys. Rev. Lett. **34** (1975) 1253.
13) R. L. Long, Jr., D. M. Cox and S. J. Smith: J. Res. Natl. Bur. Stand. Sect. A **72** (1968) 521.

14) T. J. Morgan, J. Geddes and H. B. Gilbody: J. Phys. B **6** (1973) 2118.
15) J. F. William: Phys. Rev. **150** (1966) 7.
16) F. J. de Heer, J. Schutten and H. Moustafa: Physica **32** (1966) 1768.
17) R. D. DuBois and L. H. Toburen: Phys. Rev. A **31** (1985) 3603.
18) M. Gieler, F. Aumayr, P. Ziegelwanger, H. Winter and W. Fritsch: Phys. Rev. A **43** (1991) 127.
19) W. N. Shelton and P. A. Stoycheff: Phys. Rev. A **3** (1971) 613.
20) S. W. Nagy, W. J. Savola and E. Pollack: Phys. Rev. **177** (1969) 71.
21) F. J. de Heer, J. Schutten and H. Moustafa: Physica **32** (1966) 1793.
22) L. I. Pivovar, V. M. Tubaef and M. T. Novikov: Sov. Phys. JETP **14** (1962) 20.
23) W. L. Fite, R. F. Stebbings, D. G. Hummer and R. T. Brackmann: Phys. Rev. **119** (1960) 663.
24) G. W. McClure: Phys. Rev. **148** (1966) 47.
25) J. E. Bayfield: Phys. Rev. **185** (1969) 105.
26) K-H. Schartner, R. Hippler and H. F. Beyer: J. Phys. B **10** (1977) 93.